Hindawi
Geofluids
Volume 2022, Article ID 4673073, 8 pages
https://doi.org/10.1155/2022/4673073

Research Article

Classification Prediction of Rockburst in Railway Tunnel Based on Hybrid PSO-BP Neural Network

Min Zhang

Department of Geotechnical Engineering College of Civil Engineering, Tongji University, Shanghai 200092, China

Correspondence should be addressed to Min Zhang; zhangmintju@tongji.edu.cn

Received 29 January 2022; Accepted 2 April 2022; Published 29 June 2022

Academic Editor: Meng Jingjing

Rockburst is one of the main disasters in railway tunnel construction. In order to accurately predict the rockburst intensity level of the railway tunnel, the rock stress coefficient σ_θ/σ_c, rock brittleness coefficient σ_c/σ_t, and elastic energy index W_{et} are used as evaluation indexes of rockburst intensity, and a BP neural network rockburst prediction model based on hybrid particle swarm optimization algorithm is proposed. First, 90 groups of existing rockburst examples are selected as the basic data of the mode based on the research results at home and abroad. Then, the BP neural network is improved by using particle swarm optimization (PSO) combined with the simulated annealing algorithm. The results are obtained from the training data. Based on hybrid PSO-BP neural network, the prediction model of rockburst intensity is obtained. Finally, the model is applied to the actual railway tunnel project to verify. The results show that the model takes into account individual optimization and global optimization and can correctly and effectively predict the rockburst grade of the railway tunnel, which provides a new method for rockburst prediction of the railway tunnel.

1. Introduction

Rockburst refers to the phenomenon that when the elastic strain energy of hard and brittle surrounding rock in high stress or limit equilibrium state exceeds the energy storage limit of rock mass, the excess energy is released quickly, and there is a sudden failure of rock mass adjacent to the air. Rockburst is a common geological disaster in tunnel construction, which is characterized by rock falling or popping, accompanied by sound. In serious cases, the scale of rockburst is large, which directly threatens the safety of construction equipment and personnel.

With the rapid development of railway construction in China, the proportion of tunnel engineering has gradually increased [1, 2]. In order to ensure the construction quality, construction period, investment, and personnel and equipment safety of tunnel engineering and predict the occurrence of unknown disasters such as rockburst in advance, taking corresponding measures is of great significance for the design and construction of high-stress railway tunnel [3–10]. By studying the occurrence mechanism and influencing factors of rockburst, scholars at home and abroad put forward the discrimination basis of rockburst risk level from many angles, which has laid a solid foundation for rockburst prediction theory.

In recent years, the research on rockburst prediction has developed rapidly, and a variety of rockburst prediction methods based on multifactor analysis theory and practical case analysis have been proposed one after another. Wang and Sun [11] divided different combinations, used random forest for supervised learning, established random forest prediction model, and achieved good results in rockburst classification of underground engineering; Wang et al. [6, 12] used particle swarm optimization algorithm to obtain the internal parameters of BP neural network and established PSO-BP neural network prediction model, which significantly improved the prediction accuracy of BP neural network and provided a new method for rockburst prediction; Pu et al. [13–15] proposed a sampling probability prediction method for rockburst of deep buried tunnel by combining Monte Carlo method with numerical experiment, which provides a useful reference for rockburst prediction of deep buried tunnel; Liu and Hu [16] proposed a rockburst intensity evaluation method based on the multifactor grey target

decision theory to solve the fuzziness and uncertainty of rockburst intensity grade evaluation in the case of small samples, so as to give a more accurate rockburst intensity judgment result; Liu and Zhang [17] realized the organic combination of nonlinear theory and network analysis method in rockburst prediction by analyzing representative engineering examples at home and abroad and using improved BP neural network.

However, rockburst factor analysis is a complex nonlinear problem. Most research methods are inevitably subjective and arbitrary in the determination of index weight, and some factors cannot be accurately described by method theory. In the field of machine learning, at present, there are too few actual cases in some rockburst prediction research based on machine learning, and the established model has the phenomenon of overfitting and poor generalization. Moreover, although the ordinary PSO-BP neural network is better than the traditional BP neural network, it will fall into local optimization occasionally in the training process, and the optimization process takes too long [18–20].

Based on this, the paper selects the three most representative indexes as evaluation factors and proposes a hybrid PSO-BP neural network rockburst prediction model. Through training 80 groups of actual sample data, the relationship between various factors and rockburst intensity grade is excavated, and the accuracy of the model is evaluated by 20-fold cross validation. Compared with the traditional neural network, the model can significantly improve the accuracy and convergence efficiency, and the evaluation results are more reliable.

2. Indicators and Data

2.1. Selection of Evaluation Index. According to the research results of [21–24] on rockburst, the rockburst intensity is divided into no rockburst (grade I), slight rockburst (grade II), medium rockburst (grade III), and strong rockburst (grade IV).

The mechanism of rockburst is very complex and affected by many factors. The selection of indicators needs to be considered from many aspects.

(1) Most neural network models need a lot of data to drive, so the selected rockburst index should be common, easy to measure, and recorded in the existing literature

(2) Too many indicators will not only increase the complexity of the prediction process but also increase the training time of the model and even affect the accuracy of the prediction model. Too few indicators lead to the lack of information and cannot fully reflect the conditions of rockburst. Therefore, the selected indicators should be representative and can reflect the internal and external factors affecting rockburst intensity with the least indicators. Internal factors refer to the brittleness of rock mass, compressive strength, and stored elastic energy of rock; external factors refer to the overall geological environment and environmental changes of rock mass engineering

(3) According to the main factors affecting the occurrence and intensity of rockburst, there are three different criteria: the relationship between rockburst and surrounding rock stress, the relationship between rockburst and rock lithology, and the relationship between rockburst and energy [25]. Rock stress coefficient σ_θ/σ_c refers to the ratio of the maximum tangential stress of surrounding rock to the uniaxial compressive strength of rock, which comprehensively reflects the influence of surrounding rock stress on rockburst. The greater the ratio, the more intense the rockburst; rock brittleness coefficient σ_c/σ_t is usually expressed by the ratio of rock uniaxial compressive strength and rock uniaxial tensile strength, which reflects the close relationship between rockburst and lithology. The smaller the value is, the more likely rockburst is. The elastic energy index (elastic deformation energy index) W_{et} reflects the energy characteristics of rock. It is the ratio of the elastic strain energy released by the rock block under uniaxial compression loading and unloading and the lost elastic strain energy. The greater its value, the more energy released during failure. In the actual case, the rockburst section is mainly tensile failure accompanied by shear failure, but in the rockburst examples in the existing literature, there are few records of shear strength, so it is difficult to analyze the shear strength. Therefore, it is considered that the tensile strength represents the tensile and shear mechanical properties of rock [26].

To sum up, this paper comprehensively considers the relationship between rockburst and surrounding rock stress, lithology, and rock energy and selects rock stress coefficient σ_θ/σ_c. Rock brittleness coefficient σ_c/σ_t and elastic energy index W_{et} are used as rockburst prediction indexes.

2.2. Data Sources. Rock stress coefficient σ_θ/σ_c, rock brittleness coefficient σ_c/σ_t, and elastic energy index W_{et} are common factors in tunnels and mines. Therefore, this paper collects the required sample data from the research results of underground rockburst tendency of tunnels and mines at home and abroad [27]. After screening the obtained data, the repeated samples and some mine data are eliminated. Finally, 90 rockburst example data are used as the research samples for rockburst intensity level prediction (tunnel samples account for 60%, and mine data account for 40%), the number of samples of each level in the samples is shown in Figure 1, and some data are shown in Table 1.

3. Research Method

3.1. BP Neural Network. BP neural network belongs to multilayer feedforward neural network, which includes input layer, hidden layer, and output layer. The neurons of each

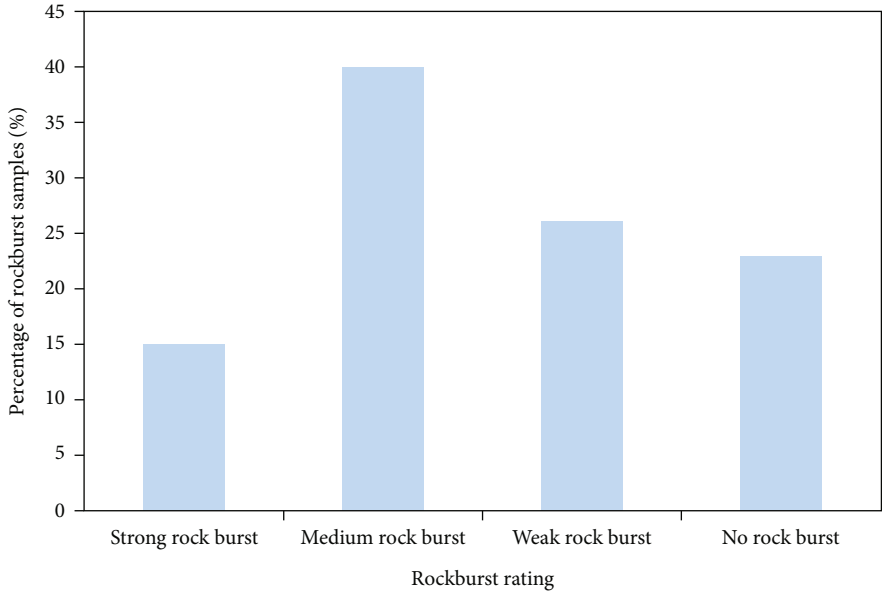

Figure 1: Proportion distribution of different rockburst grades.

layer characterize their connection strength through the size of weight and have the ability of highly nonlinear mapping. The key to determine the structure of BP neural network is the number of hidden layers and the number of neurons in hidden layers. For the selection of neural network training samples, it can be assumed that the length of the time series is L, and the data of the first N times of the series can be used to predict the data of the next M times. That is, divide the whole time series into K overlapping data samples with a length of $N + M$, so as to obtain $K = L - (N + M) + 1$ training sample. The first N values of each sample are the input layer, and the last M values are the output layer. By learning the training samples for many times, a high-precision network model is generated.

3.2. Principle of PSO Algorithm Based on Simulated Annealing. Particle swarm optimization (PSO) is an algorithm inspired by the foraging behavior of birds, which is called particle swarm optimization for short. Particle swarm optimization algorithm is suitable for optimization in dynamic multiobjective environment. It can converge to the optimal solution faster and with greater probability and can take into account the individuality and globality. Its disadvantage is that in the process of function optimization, it mainly depends on the individual information and global information between particles to constantly update the position and speed of particles, so that the particles gradually approach the optimal solution. Therefore, PSO algorithm is easy to precocious, and the convergence speed in the later stage is slow.

Simulated annealing algorithm is an intelligent algorithm to find the global optimal solution of the optimization problem by simulating the annealing process of high-temperature objects. The basic idea is as follows: first, an initial solution is generated as the current solution, and then, in the field of the current solution, a nonlocal optimal solution is selected with probability, and the solution is repeated, so as to ensure that it will not fall into the local optimal solution. Simulated annealing is a kind of search process, which introduces the green algorithm with random factors. It accepts a solution worse than the current solution with a certain probability. Therefore, it may jump out of the local optimal solution trap and converge to the global optimal solution region, with high search accuracy.

In this paper, simulated annealing algorithm and particle swarm optimization algorithm are combined to form a hybrid particle swarm optimization (SA-PSO) algorithm [28]. The hybrid algorithm is dominated by the operation flow of basic particle swarm optimization algorithm. In the process of particle update speed and position, simulated annealing mechanism is added to learn from each other. Compared with a single algorithm, hybrid particle swarm optimization algorithm is not prone to premature convergence, and the convergence speed has been significantly improved, which improves the overall performance of the algorithm. Specific steps are as follows:

(1) Randomly set the speed and position of each particle

Assuming that there are N individuals in the D-dimensional space, the location and speed of the position and velocity of the i-th individual are defined as follows:

$$X_i = \left(x_i^1, x_i^2, \cdots, x_i^k, x_i^d\right), \tag{1}$$

$$V_i = \left(v_i^1, v_i^2, \cdots, v_i^k, v_i^d\right), \tag{2}$$

where x^k is the position of the i individual in the k -dimensional space and v^k is the velocity of the i individual in the k-dimensional space.

Table 1: Partial rockburst data.

Serial number	σ_θ/σ_c	σ_c/σ_t	W_{et}	Grade
1	0.38	27.96	6.9	III
2	0.15	29.63	7.2	I
3	0.18	30.12	7.3	I
4	0.24	26.36	7.4	II
5	0.12	22.36	6.3	I
6	0.19	28.63	7.5	I
7	0.79	20.36	4.3	III
8	0.34	25.63	6	II
9	0.28	26.21	6.2	II
10	0.38	23.1	7.8	IV
11	0.25	26.3	5.5	III
12	0.31	27.1	6.8	I
13	.0.28	23.6	7.1	III
14	0.30	24.6	6.9	III
15	0.26	23.9	6.5	III
16	0.19	25.4	6.1	IV
17	0.24	27.4	6.2	I
18	0.38	25.8	6.9	III
19	0.41	24.3	6.6	IV
20	0.52	28.4	6.4	IV
…	…	…	…	…
81	0.53	8.77	4.9	III
82	0.41	19.65	6.1	III
83	0.35	19.23	4.1	II
84	0.38	23.4	4.1	II
85	0.32	18.23	4.6	II
86	0.28	19.63	4.3	II
87	0.48	8.67	2.7	II
88	0.42	19.68	7.5	IV
89	0.47	9.05	5.2	III
90	0.24	20.38	5.6	II

(2) Save individual extremum and global extremum

The fitness values of each particle are evaluated, and the location and fitness of particles are saved as the individual extreme Best_p of particles. The best extreme values of all extreme values of individuals are preserved as global extreme values Best_p.

(3) Determine the initial temperature

The following algorithm is used for the initial temperature and desuperheating method.

$$T_{t+1} = \lambda T_t (0 < \lambda < 1, t = 0, 1, \cdots, M), \tag{3}$$

$$T_0 = \frac{\text{Best}_g^0}{\ln 5}, \tag{4}$$

where T_t is the initial temperature of iteration $t+1$, λ is the inertia weight of annealing constant, and M is the total number of iterations.

(4) Determine the fitness value of each particle at the current temperature

$$TF\left(X_i^t\right) = \frac{e^{-\left(f\left(X_i^t\right)-\text{best}_g^t\right)/T_t}}{\sum_{i=1}^{N} e^{-\left(f\left(X_i^t\right)-\text{best}_g^t\right)/T_t}}. \tag{5}$$

Among them, $TF(X^t{}_i)$ is the fitness value corresponding to the i-th particle in the t-thiteration, $\text{best}^t{}_g$ is the global optimal extremum in the t-th iteration, and N is the number of initial particles.

(5) Update position and speed

Determine the globally optimal alternative value X_i' under annealing conditions from all X_i, and update the position and speed of the following 2 formulas.

$$\begin{aligned} x_i^k(t+1) &= x_i^k(t) + v_i^k(t+1), \\ v_i^k(t+1) &= \eta \bullet v_i^k(t) + c_1 r_1 \left[p_i^k - x_i^k(t)\right] + c_2 r_2 \left[p_{gt}' - x_i^k(t)\right], \\ \eta &= \frac{2}{2 - (c_1 + c_2) - \sqrt{(c_1 + c_2)^2 - 4(c_1 + c_2)}}, \end{aligned} \tag{6}$$

where $v_i{}^k(t)$ is the velocity of the particle in the t iteration, $x_i^k(t)$ is the position of the particle in the t iteration, $p_i{}^k$ is the particle corresponding to the extreme value of a single individual, p_{gy}' is the globally optimal substitution value in the t iteration under simulated annealing, c_1 and c_2 are the learning factor, and η represents the weight.

(6) Compare the current Best_p and Best_p, update Best_p, and then use equation (3) to desuperheat

(7) When the stop condition is reached, the result is output; otherwise, return to step (4) to continue the search

3.3. Rockburst Prediction Model Based on Mixed PSO-BP. The rockburst grade prediction model proposed in this paper is established based on matlab2018b. Firstly, the center of BP neural network is obtained by K-means clustering method, and then, the simulated annealing algorithm is applied to particle swarm optimization algorithm to optimize the internal parameters of BP neural network. Finally, the rockburst grade prediction model of hybrid PSO-BP neural network is trained.

3.3.1. Sample Segmentation. According to the common partition methods of machine learning, the samples are divided into test set and training set in the proportion of 4 : 1. The

Table 2: Actual rating and indicator data of tunnel to be predicted.

Sample number	Rock type	Buried depth/m	σ_θ/σ_c	σ_c/σ_t	W_{et}	Actual grade
Q-1	Limestone	498	0.325	9.23	1.968	II
Q-2	Limestone	403	0.468	9.68	3.865	III
Q-3	Basalt	695	0.523	14.36	4.325	III
Q-4	Limestone	640	0.576	11.85	2.325	II
Q-5	Limestone	640	0.765	16.85	3.236	III

training set is used for model training and updating parameters; the test set is used to test the accuracy of the model, adjust parameters (number of cluster centers, number of iterations, learning rate, etc.), monitor whether the model has been fitted, evaluate its generalization ability, and test its real prediction accuracy after the final training of the model.

3.3.2. Model Input and Output. The input sample data is normalized with mapminmax command, and the normalized sample interval is [0,1], which makes the data dimensionless and speeds up the convergence speed. Model training sample output uses "1," "2," "3," and "4" to represent four levels of rockburst (no rockburst level I, slight rockburst level II, intermediate rockburst level III, and strong rockburst level IV). The test sample output results are rounded with the round function.

3.3.3. Hidden Layer Node Determination. Theoretically, the number of hidden layer nodes increases, which can make the radial basis function neural network achieve arbitrary accuracy. However, in practical application, too many hidden layer nodes will lead to the increase of algorithm training time and learning cost and reduce the generalization ability and fault tolerance of the model, resulting in overfitting. In this paper, the hidden layer of BP neural network is one layer, and the number of neuron nodes is calculated by BP neural network based on K-means clustering. When the clustering center is 20, a good approximation effect can be achieved. Therefore, the number of hidden layer nodes is 20, and the center (c_i) of BP is 20 clustering center C obtained by K-means clustering.

3.3.4. Construct Fitness Function. The performance of neural networks is usually measured by mean square error (MSE) [28]. In this paper, the calculation formula of neural network mean square error MSE is selected as the fitness calculation function of particle swarm optimization algorithm. The mixed particle swarm optimization algorithm is used to calculate the weight and basis function standard deviation under the minimum mean square error, which is the optimal parameter of the model.

$$\mathrm{MSE} = \frac{1}{n}\left(\tilde{y}_p - y_p\right)^2. \tag{7}$$

$\tilde{y}_p$ is the model output value; y_p is the expected value of the model.

Table 3: Rockburst data and prediction results of Laobishan tunnel.

Sample number	Actual grade	Model prediction level		
		Hybrid PSO-BP	PSO-BP	BP
Q-1	II	II	II	II
Q-2	III	III	III	II
Q-3	III	III	III	III
Q-4	II	II	III	III
Q-5	III	III	III	III

3.3.5. Calculate the Optimal Weight. Set the basic parameters of SA-PSO algorithm: the learning factors c_1 and c_2 are all 0.5, the initial population number $N = 200$, the maximum number of iterations $M = 60$, and the cooling rate $\lambda = 0.85$.

X and V are one-dimensional vectors, $V = (v_1, v_2, \cdots, v_{40})$, and $X = (w_1, w_2, \cdots, w_{20}, \sigma_1, \sigma_2, \cdots, \sigma_{20})$. Randomly take $N = 200$ different X and V with randn function, and iteratively optimize $M = 60$ times according to the steps shown in Section 2.2 to obtain the optimal weight W and standard deviation σ.

3.3.6. Model Output. The output of hybrid PSO-BP neural network can be obtained by equations (2) and (3).

3.3.7. Cross Validation. In this paper, the cross validation method is used for model training and accuracy evaluation.

The training set and test set are brought into the model for 20 times of training and testing, and the training set and test set are randomly divided according to the ratio of 4 : 1 each time; the minimum value of fitness function, global optimal weight$W$, and variance were obtained after each model trainingσ, and record the accurate classification rate of test set samples and the mean square error of test set samples; after the training, the average of the accurate classification rate and mean square error of 20 test sets are taken as the actual accuracy and mean square error of the model in this paper; finally, the model whose accuracy and mean square error are closest to the average value is selected as the prediction model of tunnel rockburst tendency. This method can effectively avoid the overfitting phenomenon and obtain the best prediction model. Through cross validation, the average mean square error (the average minimum value of fitness function) of the sample training set is 0.048, the average mean square error of the test set is 0.124, and the accuracy is 95.98%. The W of the best model is selected according to the average value σ[29–33].

3.3.8. Model Comparison. The expansion speed of radial basis function and the maximum number of neurons of ordinary BP neural network need to be set by experience. It is greatly affected by human factors and is prone to overfitting, resulting in high classification error rate of test set and unable to accurately predict the rockburst intensity level.

The test results of ordinary PSO-BP model are unstable. The mean square error of training set is 0.07~0.12, the mean square error of test set is 0.24~0.45, the accuracy is

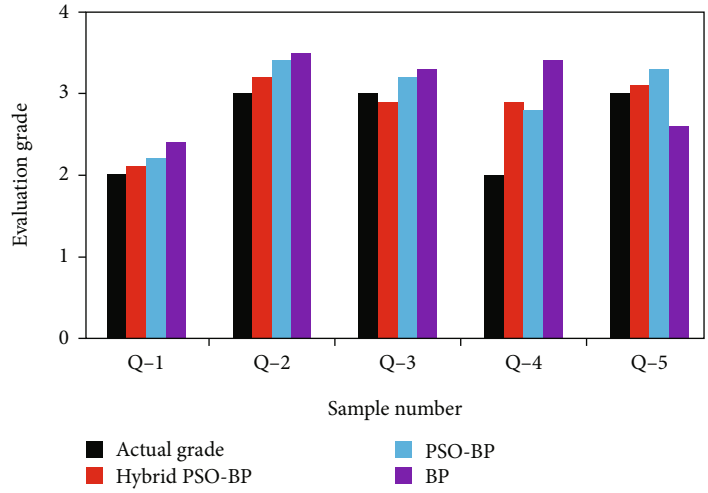

Figure 2: Comparison of model output.

84.36%~96.35%, and the number of iterations is more than 70.

The parameters of the hybrid PSO-BP model proposed in this paper are less. In each training process, the number of iterations reaches 35 times and then converges to the minimum value. The mean square error of the training set is between 0.06 and 0.08, and the mean square error of 16 test set samples is less than 0.4. After 20 training, the average minimum value of fitness function is 0.053, and the average accuracy of test set is more than 97.26%. Through comparison, it can be seen that the training process of hybrid PSO-BP model will avoid falling into local optimization to a great extent, with faster convergence, shorter time-consuming, and significantly improved accuracy.

4. Engineering Application

4.1. Project Overview and Application. Daliangshan tunnel is located in the south of Sichuan Province and belongs to the transition zone between the first and second terraces in China. It is a double track tunnel with a total length of 12564 m. The tunnel belongs to structural denudation landform of Dadu River Canyon, with ground elevation of 600~1256 m and maximum buried depth of about 698 m. The tunnel site is a monoclinal structure, the rock bedding is N25°E/18°NW, and steep joints are developed mainly N40°W/65°NE and N50°E/90°. The reverse faults are developed in the area. The reverse fault intersects with the line at D1K245+286, the fault strike is N65 ~75°E, the dip angle is 40°, and the fault offset is unknown. The hanging wall of the fault is basalt formation, and the footwall is sandstone, mudstone, and shale formation. The construction of the tunnel mainly based on the new Austrian tunneling method. There are altogether 3 transverse holes in the tunnel. The length of No. 1 transverse hole is 900 m, the largest buried depth is 498 m, the No. 2 transverse hole is 1768 m, the maximum buried depth is 691 m, the No. 3 transverse hole is 1768 m, and the maximum depth is 605 m.

Due to the basalt, limestone, and other hard rocks along the Daliangshan tunnel, the rock mass integrity is good, and the compressive strength is high. It has good elasticity and brittleness, so the tunnel is very prone to rockburst during construction. In this paper, the experimental data of three rockburst sections in the construction of transverse tunnel of Daliangshan tunnel are taken as analysis samples of which two occur in limestone and the other in basalt. At D1K245 +645, the buried depth of the tunnel is 498 m, the maximum principal stress is 25.6 MPa, the maximum tangential stress is 33.45 MPa, and the average free immersion saturated compressive strength of limestone here is 62~73 MPa. The rock structural joints are relatively developed, and the rock mass is fresh and hard. During tunnel construction, the plate limestone often peels off under the control of structural joints and the influence of in situ stress. At D1K245+286, the buried depth of the tunnel is 403 m, the maximum principal stress is 14.98 MPa, the maximum tangential stress is 23.65 MPa, and the uniaxial compressive strength of the limestone here is 69.32 MPa. In the actual construction, the rock block has small-scale peeling. Near D1K203+435, the depth is 640~695 m, the maximum principal stress is 49.2~56.2 MPa, and the maximum tangential stress is 60.85~82.36 MPa. The joints of basalt and limestone are relatively developed, and the rock mass is dry. Rockburst sound, stone ejection, and rock mass collapse occur in the actual construction. Detailed data are shown in Table 2.

4.2. Results and Discussion. Five sample points of rockburst in Daliangshan tunnel of reconstructed railway are taken and predicted by mixed PSO-BP model, PSO-BP model, and ordinary BP model, respectively. The prediction results are shown in Table 3.

(1) The mixed PSO-BP neural network model correctly predicted five samples, and the samples predicted by PSO-BP model and ordinary BP were wrong

(2) Comparing the output results of the three models (Figure 2), the error between the actual output result

and the expected output result (actual level) of the hybrid PSO-BP neural network prediction model is the smallest

It can be seen that the RBF neural network optimized by the hybrid algorithm of simulated annealing algorithm and particle swarm optimization algorithm has strong antinoise and repair ability, can largely eliminate the interference of abnormal data and wrong data in the training set, and accurately predict the rockburst intensity level.

5. Conclusion

(1) By referring to relevant literature, the rock stress coefficient is selected σ_θ/σ_c. Rock brittleness coefficient σ_c/σ_t and the elastic index W_{et} are used as the evaluation index of rockburst intensity

(2) The radial basis function neural network optimized by hybrid particle swarm optimization is not only faster than the ordinary PSO-BP model but also can avoid the influence of noise data, and the accuracy is 95.98%

(3) The advantages of artificial intelligence in data processing have been gradually revealed. Processing data through machine learning method can more objectively and accurately reflect the impact of various factors on rockburst intensity

Data Availability

The data used to support the finding of this study are included in the article.

Conflicts of Interest

The author declares that there are no conflicts of interest regarding the publication of this paper.

Authors' Contributions

Min Zhang carried out the experiments, analyzed the results, and conducted the theoretical explanations, as well as wrote the manuscript.

Acknowledgments

The author would like to express appreciation to Department of Geotechnical Engineering College of Civil Engineering, Tongji University for providing the laboratory.

References

[1] H. Wu, G. Zhao, and S. Ma, "Failure behavior of horseshoe-shaped tunnel in hard rock under high stress: phenomenon and mechanisms," *Transactions of Nonferrous Metals Society of China*, vol. 32, no. 2, pp. 639–656, 2022.

[2] S. Li, Y. G. Zhang, M. Y. Cao, and Z. N. Wang, "Study on excavation sequence of pilot tunnels for a rectangular tunnel using numerical simulation and field monitoring method," *Rock Mechanics and Rock Engineering*, vol. 1, no. 5, 2022.

[3] Z. Zhu and H. Zhang, "Study on hazard prediction of rock burst based on GA-ELM," *Journal of Safety Science and Technology*, vol. 10, no. 8, pp. 46–51, 2014.

[4] J. Zhou, X. B. Li, and X. Z. Shi, "Long-term prediction model of rockburst in underground openings using heuristic algorithms and support vector machines," *Safety Science*, vol. 50, no. 4, pp. 629–644, 2012.

[5] Y. G. Xue, C. H. Bai, D. H. Qiu, F. M. Kong, and Z. Q. Li, "Predicting rockburst with database using particle swarm optimization and extreme learning machine," *Tunnelling and Underground Space Technology*, vol. 98, p. 103287, 2020.

[6] J. Q. Wang, B. Prabhat, and M. Shakil, "Review of machine learning and deep learning application in mine microseismic event classification," *Mineral Deposits*, vol. 15, no. 1, pp. 19–26, 2021.

[7] X. L. Ma, J. G. Li, Z. H. Wang et al., ""Experimental study on vibration reduction technology of hole-by-hole presplitting blasting"," *Geofluids*, vol. 2021, Article ID 5403969, 10 pages, 2021.

[8] B. Yang, M. He, Z. Zhang, J. Zhu, and Y. Chen, "A new criterion of strain rockburst in consideration of the plastic zone of tunnel surrounding rock," *Rock Mechanics and Rock Engineering*, vol. 55, no. 3, pp. 1777–1789, 2022.

[9] M. He, Z. Zzhiqiang, Z. Jiwei, and L. Ning, "Correlation between the constant mi of Hoek-Brown criterion and porosity of intact rock," *Rock Mechanics and Rock Engineering*, vol. 11, no. 10, 2021.

[10] M. He, Z. Q. Zhang, J. W. Zhu, N. Li, G. Li, and Y. S. Chen, "Correlation between the rockburst proneness and friction characteristics of rock materials and a new method for rockburst proneness prediction: field demonstration," *Journal of Petroleum Science and Engineering*, vol. 205, p. 108997, 2021.

[11] Y. Wang and S. Sun, "Prediction of rock burst risk rating based on grid search and ELM," *China Safety Science Journal(CSSJ)*, vol. 27, no. 8, pp. 97–101, 2017.

[12] J. Wang, T. Zuo, X. Li, Z. Tao, and J. Ma, "Study on the fractal characteristics of the pomegranate biotite schist under impact loading," *Geofluids*, vol. 2021, Article ID 1570160, 8 pages, 2021.

[13] Y. Y. Pu, D. B. Apel, and C. Wei, "Applying machine learning approaches to evaluating rockburst liability: a comparation of generative and discriminative models," *Pure and Applied Geophysics*, vol. 176, no. 10, pp. 4503–4517, 2019.

[14] Y. Y. Pu, D. B. Apel, C. Wang, and B. Wilson, "Evaluation of burst liability in kimberlite using support vector machine," *Acta Geophysica*, vol. 66, no. 5, pp. 973–982, 2018.

[15] Y. Y. Pu, D. B. Apel, and R. Hall, "Using machine learning approach for microseismic events recognition in underground excavations: comparison of ten frequently-used models," *Engineering Geology*, vol. 268, p. 105519, 2020.

[16] Y. R. Liu and S. K. Hu, *Information Technology in Geo-Engineering*, A. G. Correia, J. Tinoco, P. Cortez, and L. Lamas, Eds., Springer International Publishing Ag, Cham, 2020.

[17] H. Liu and X. J. Zhang, "Predictive analysis of impact hazard level of coal rock mass based on fuzzy inference network," *Journal of Intelligent Fuzzy Systems*, vol. 38, no. 2, pp. 1509–1518, 2020.

[18] H. Liu, F. Xu, B. Liu, and M. Deng, "Time-series prediction method for risk level of rockburst disaster based on CNN-

LSTM," *Journal of Central South University of Science and Technology*, vol. 52, no. 3, pp. 659–670, 2021.

[19] Y. Lin, K. P. Zhou, and J. L. Li, "Application of cloud model in rock burst prediction and performance comparison with three machine learnings algorithms," *IEEE Access*, vol. 6, pp. 30958–30968, 2018.

[20] W. Z. Liang, A. Sari, G. Y. Zhao, S. D. McKinnon, and H. Wu, "Short-term rockburst risk prediction using ensemble learning methods," *Natural Hazards*, vol. 104, no. 2, pp. 1923–1946, 2020.

[21] T. Z. Li, Y. X. Li, and X. L. Yang, "Rock burst prediction based on genetic algorithms and extreme learning machine," *Journal of Central South University*, vol. 24, no. 9, pp. 2105–2113, 2017.

[22] N. Li, L. Wang, and M. Jia, "Rockburst prediction based on rough set theory and support vector machine," *Journal of Central South University of Science and Technology*, vol. 48, no. 5, pp. 1268–1275, 2017.

[23] N. Li, R. Jimenez, and X. D. Feng, *Isrm European Rock Mechanics Symposium Eurock 2017*, P. Konicek, K. Soucek, and P. Konecny, Eds., vol. 191, Elsevier Science Bv, Amsterdam, 2017.

[24] N. Li, X. D. Feng, and R. Jimenez, "Predicting rock burst hazard with incomplete data using Bayesian networks," *Tunnelling and Underground Space Technology*, vol. 61, pp. 61–70, 2017.

[25] M. Lan, Z. Liu, and F. Feng, "Attempt to study the applicability of the online sequential extreme learning machine to the rock burst forecast," *Journal of Safety and Environment*, vol. 14, no. 2, pp. 90–93, 2014.

[26] Y. Geng, L. L. Su, Y. H. Jia, and C. Han, "Seismic events prediction using deep temporal convolution networks," *Journal of Electrical and Computer Engineering*, vol. 2019, Article ID 7343784, 14 pages, 2019.

[27] S. Afraei, K. Shahriar, and S. H. Madani, "Developing intelligent classification models for rock burst prediction after recognizing significant predictor variables, section 2: designing classifiers," *Tunnelling and Underground Space Technology*, vol. 84, pp. 522–537, 2019.

[28] Y. G. Zhang, J. Tang, Y. M. Cheng et al., "Prediction of landslide displacement with dynamic features using intelligent approaches," *International Journal of Mining Science and Technology*, vol. 2, no. 1, pp. 1–11, 2022.

[29] X. L. Li, Z. Y. Cao, and Y. L. Xu, "Characteristics and trends of coal mine safety development," *Energy Sources, Part A: Recovery, Utilization, and Environmental Effects*, vol. 20, no. 5, 2020.

[30] X. L. Li, S. J. Chen, Q. M. Zhang, X. Gao, and F. Feng, "Research on theory, simulation and measurement of stress behavior under regenerated roof condition," *Geomechanics and Engineering*, vol. 26, no. 1, pp. 49–61, 2021.

[31] W. Zhong, J. Ouyang, D. Yang, X. Wang, Z. Guo, and K. Hu, "Effect of the in situ leaching solution of ion-absorbed rare earth on the mechanical behavior of basement rock," *Journal of Rock Mechanics and Geotechnical Engineering*, vol. 30, no. 15, 2022.

[32] X. L. Li, S. J. Chen, S. M. Liu, and Z. H. Li, "AE waveform characteristics of rock mass under uniaxial loading based on Hilbert-Huang transform," *Journal of Central South University*, vol. 28, no. 6, pp. 1843–1856, 2021.

[33] X. L. Li, S. J. Chen, S. Wang, M. Zhao, and H. Liu, "Study on in situ stress distribution law of the deep mine taking Linyi Mining area as an example," *Advances in Materials Science and Engineering*, vol. 2021, Article ID 5594181, 11 pages, 2021.